Iranian Journal of Chemical Engineering

Journal Homepage: www.ijche.com

pISSN: 1735-5397
eISSN: 2008-2355

Regular Article

Investigating the Effect of the Structural Parameters of Mixed Matrix Membranes on Their Effective Gaseous Penetrant Diffusion Ratio Using CFD Tools

M. Morovat [1], ***O. Bakhtiari*** [1,2*]

[1] *Membrane Research Center, Faculty of Petroleum and Chemical Engineering, Razi University, Kermanshah, Iran*
[2] *Membrane Research Center, Advanced Research Center for Chemical Engineering, Faculty of Petroleum and Chemical Engineering, Razi University, Kermanshah, Iran*

ARTICLE INFO

Article history:
Received: 2023-02-01
Accepted: 2023-03-06
Available online: 2023-03-12

Keywords:
Mixed Matrix Membranes (MMMs),
Gas Separation,
Effective Diffusivity,
Simulation,
CFD,
Finite Element Method (FEM)

ABSTRACT

The ability and competitiveness of the membrane processes for gas separation are evaluated by their membranes' permeability and selectivity where it has been tried to enhance both in the promising generation of mixed matrix membranes (MMMs). In the current study, two-and-three-dimensional models were constructed for MMMs, and the Fick's first law was solved numerically for them by using the Finite Element Method (FEM) and Computational Fluid Dynamic (CFD) tools. The effects of different MMMs' structural parameters – such as the volume fraction, size and mode of packing, i.e. regular or random – of the filler particles on the effective permeability of the pure gaseous penetrants through the MMMs were investigated. Furthermore, the interfacial equilibrium constant of the penetrants and their diffusivity ratios were also evaluated from the viewpoint of their impacts on the MMMs' separation performance. Some well-known established models including Maxwell, Bruggeman, Lewis - Nielsen, Pal, and Chiew - Glandt were applied in the modeling. The deviation of the simulation results from the experimentally measured ones was low enough, however, at higher loadings of the filler particles, the simulation deviation became greater. the results of the simulation through PSF - MCM-41 MMMs were compared with those of experimentally measured ones and the AAREs of 31.0 (The lowest deviation), 42.7, and 41.0 % were obtained for CO_2, O_2, and N_2, respectively.

DOI: 10.22034/ijche.2023.384122.1475 URL: https://www.ijche.com/article_168307.html

1. Introduction

Today, the necessity of operational separation

*Corresponding author: obakhtiari@razi.ac.ir (O. Bakhtiari)

units is approved in different industrial processes such as oxygen-nitrogen separation, natural gas separation, etc. [1]. Using membranes is considered a fast-growing technology compared with almost all other conventionl gas separation processes. Therefore, nowadays membrane processes attract a lot of attention and various materials are used for the preparation of gas separation membranes. Among them, the polymeric membranes were used for gas separation tasks in different processes, such as natural gas purification [2-4].

In 1991, Robeson, after the investigation of different published data, pointed out that the polymeric membranes had a trade-off between their selectivities and permeabilities for specific gas pairs where they were limited to an upper bound limit, which was known as the Robeson upper bound limit after him and updated in 2008 [5]. According to this limit, as the membrane permeability increases, its selectivity for a given gas pair decreases and vice versa. The enhancement of the separation performance is the goal of many research activities in the membrane field to overcome this limitation via different approaches such as extending different polymerization techniques for modification of the volume or surface of the membrane structure [6, 7], the preparation of mixed matrix membranes (MMMs) in which proper inorganic filler particles are incorporated in polymeric matrices [8-10], and/or the preparation of composite membranes [11, 12].

As mentioned above, MMMs are the new generations of membranes that try to overcome the shortcomings of the polymeric membranes for different industail applications. In this type of membranes, inorganic filler particles are incorporated into the continuous phase of the polymer as the dispersed phase. The inorganic filler particles are usually selected due to their high separation properties for the enhancement of the resultant MMMs, however, some undesired defects, such as the fragility of the resultant MMMs (i.e., low processability) [13], void formation [14, 15] or polymeric matrix chain rigidification at the filler particles' surface [14], fully or partially blocked pores of the filler particles [16, 17], may prevent the goal of the enhancement of the separation performance or their applicability. Experimental studies to study the structur and separation performance of MMMs are money and time-consuming. Meanwhile, the mathematical modeling and simulation using different developed efficient software can be great potential aids for the reduction of the money and time consumption in the investigation of MMMs and also for better designing MMMs. MMMs permeation predictive models are used for their effective permeability prediction for gaseous penetrants.

The Maxwell model was originally presented in 1873 to predict the electrical conductivity of homogeneous environments [18] and then altered for the prediction of the MMMs' separation. The Maxwell model is limited to the low volume fractions of filler particles (i.e., < 20 %). To calculate the MMMs' permeability at higher volume fractions of the filler particles, the Bruggeman model can be employed [14]. This model considers the impact of the loadings of filler particles higher than those in dilute suspensions of randomly dispersed spherical particles via a trial-and-error procedure of solving. Also, in this model, as in the Maxwell model, the MMMs' permeabilities cannot be predicted at the maximum packing volume fraction of filler particles.

In recent years, other analytical methods such as the Lewis - Nielsen, the Chiew -

Glandt, the Pal, and some other models have been developed and/or adapted for the prediction of the MMMs' permeability, where the effect of some other parameters, like the effect of the filler particles' size and MMMs' structural defects on their permeabilities are considered [14]. The Lewis-Nielsen model involves the impact of the morphology of the MMM on its permeability via ϕ_m which is the maximum inorganic spherical filler particles volume fraction randomly filled in a matrix and equals 0.64. The Pal model, like the Bruggeman model, must be solved by a trial-and-error procedure to calculate P_M. The mathematical equations of the above-mentioned models are presented in Table 1 where P_M, P_c, and P_d are the effective permeabilities of gaseous penetrants through the MMM, the matrix phase, and the incorporated particles respectively, and ϕ is the volume fraction of the dispersed phase.

Table 1
Some MMMs' permeability prediction models.

Model	Equation	Ref.
Maxwell	$P_M = P_c \frac{P_d + 2P_c - 2\phi_d(P_c - P_d)}{P_d + 2P_c + \phi_d(P_c - P_d)}$	[18]
Bruggeman	$\left(\frac{P_M}{P_c}\right)^{-1/3} \frac{P_M/P_c - P_d/P_c}{1 - P_d/P_c} = 1 - \phi_d$	[19]
Lewis - Nielsen	$P_M = P_c \frac{1 + 2\,(P_d/P_c - 1)/(P_d/P_c + 2)\,\phi_d}{1 - (P_d/P_c - 1)/(P_d/P_c + 2\phi_d)\,\psi}$	[20]
Polyolefin plant	$\psi = 1 + \left(\frac{1 - \phi_m}{\phi_m^2}\right)\phi_d$	[30]
Pal	$\left(\frac{P_M}{P_c}\right)^{1/3} \frac{(P_d/P_c) - 1}{(P_d/P_c) - (P_M/P_c)} = \left(1 - \frac{\phi}{\phi_m}\right)^{-\phi_m}$	[21]

Recently, various simulations have been made on the MMMs for the prediction of different gas separations. In 2012, Marand et al. studied the impact of the solubility partition coefficient on the effective diffusivity of the MMM. They used the Davis model to predict the effective diffusivity on CO_2 [23-25]. Their calculated CO_2 effective diffusivity by using extending effective medium (EMT) were compared to those experimentally measured by the calculated AARE of 89 % [26]. They showed the MMM Systems with the partition coefficient values (K) greater than unity will indicate a decrement in diffusivity as the volume fraction of filler particles increases. Furthermore, the selectivity and permeability of MMMs which have K values smaller than unity, enhance only at the loadings of the dispersed phase particles higher than the percolation threshold [26].

In 2013, Singh et al. predictied MMMs separation performance by application the FEM method of CFD. They investigated the solubility of CO_2 and the diffusivity data in ZIF-8 as filler and PDMS, 6FDA-DAM-15 %, etc. for simulation [27]. Their simulation results indicated the effects of the partition coefficients between the phases of the matrix and the filler particles, diffusivity ratio, and filler size. The results of their studies revealed that in an ideal MMM structure, the particles size of the filler has no significant effect on the

diffusion of the effective MMMs. They also showed that as the diffusivity ratio increased from 10 to 1000 in K = 1, the effective diffusivity ratio would increase by 30 %. Furthermore, they also indicated that the partition coefficient played a more effective role in MMMs' separation performance: for instance at a volume fraction of 0.5 for the filler particles, the effective diffusivity of the MMM increased from 3.5 to 5.6 as the partition coefficient increased from 1 to 100, [27].

In 2015, Gheimasi et al. investigated a novel model for the prediction of the permeability of the gaseous penetrants through the MatrimidPP-CMS and zeolite 4A-PVAc MMMs. In their model, the effects of the filler particles' shape and also unwanted defects that might occur around the filler particles were considered. They compared the predicted permeability with the experimentally measured data and found AARE as about 0.73 - 31.53 % [28].

In 2015, Wang et al. investigated a three-dimensional mass transport simulation for the prediction of the effective diffusivity of the MMMs containing tubular filler particles. In their models, the diffusion equation of Fick's law was solved to find the concentration profile of penetrants inside the MMMs. Also, the effects of different structural parameters, the volume fraction of the tubular filler particles, and their spatial configuration, alignment, aspect ratio, and diffusivity ratio, were investigated. They understood that the orientation and spatial distribution of the tubular filler particles had significant impacts on the MMMs' mass transport. They also found that the filler configuration within the structure of MMMs considerably affected their effective diffusivity. They showed that as θ increased, the ratio of D_{eff}/D_m decreased to less than 1 at $\theta \approx 45$ ° for the $D_f/D_m = 5$. And the maximum D_{eff}/D_m appeared at $\theta = 10$ °. They justified the result due to maximizing the effectiveness of penetrant mass transport length as the filler particles oriented at 10 °. And finally, the filler particles with higher diffusivity ratios can improve the MMMs' effective diffusivity [29].

Furthermore in 2015, Yang et al. presented a numerical technique for the prediction of effective diffusivity in hollow fiber mixed matrix membranes (HFMMMs). They investigated some parameters such as the filler particles' size and diffusivity, the solubility of the penetrants in the matrix and the filler particles phase of the HFMMM, and the inner diameter and thickness of the fiber top layer. Their model outcomes revealed that as the diffusivity and solubility of filler particles and the thickness of the fiber's top layer increased, and also as the size of the filler particles and the inner diameter of the fibers decreased, the resulting HFMMMs' diffusivity incremented. For instance, the results of their investigations showed that as D_f/D_m increased from 10 to 10^3, the effective diffusivity in the HFMMM was improved from 3.1 to 5.7. Their simulation results revealed an acceptable agreement with experimentally measured data at the lower filler loading, i.e., AARE of 47 % [30].

In 2017, Monsalve-Bravo et al. presented a new model for the approximation of the effective permeability of pure gaseous penetrants through MMMs. The MMM flux was estimated by EMT. The results of their work revealed that an increment in the filler particle size decreased the effective permeability of the MMM due to the increased interfacial area of the polymer-filler particles . Their predicted values were in very good agreement with the experimentally observed data, especially in the low-volume fractions of

the filler particles. Furthermore, the effect of the filler packing was investigated. The random structure has a higher effective permeability compared with that of the regular structure of MMMs. This can be attributed to the higher permeability pathways provided by the filler particles compared with those in the pristine polymer regions near the filler particles of the regular structure [31].

In 2018, Rajati et al. used a theoretical model to estimate the permeability of the O_2, N_2, CO_2, CH_4, N_2O, and Ar penetrant through the zeolite 4A as the filler particles of MMMs. The results they got for the amounts of the permeability of AREs of N_2 and CH_4 through 4A zeolite were 4.3 and 6.9 % respectively. They also reported the AREs of the O_2 permeability of MMMs using the modified Felske and the Maxwell models as 1.2 and 55.6 % respectively. Furthermore, the AREs of the predicted CO_2 permeability through the DDR and silicalite-1 zeolitic filler particles incorporated MMMs were calculated as 0.7 and 1.8 % for Bruggeman's and Maxwell's models respectively [32].

All above-mentioned models and the research associated with them consider the packing of the filler particles within the MMMs structure via such adjusting parameter(s) as ϕ_m in the Pal model; however, CFD tools provide more insights to the MMM's structural feactures and then their structure-related properties like permeabilities. In this study, the effective permeability of MMMs was estimated based on a numerical simulation. Employing CFD tools enabled us to consider the actual situations which might occure in the MMMs' structure, such as the packing regularity, size, and loading of the filler particles and their impact on the MMMs' separation performance, as the novel aspect of the study, which has not been provided by currently available analytical models. Two-and-three-dimensional models were constructed for different loadings of filler particles incorporated within MMMs and after that the mass transfer through the MMMs was simulated by the CFD software and, finally, the concentration profile of the gaseous penetrants was determined. The effects of the partition coefficient of the interfacial concentration between the polymer matrix and the filler particles and also the size of the filler particles were evaluated. Finally, the results of the CFD simulation were compared with the results of EMT and the experimental data.

2. Models and methods

2.1. Physical model and constructed geometric structure of MMMs

In the current study, the effective diffusion coefficients of carbon dioxide (CO_2), oxygen (O_2), and nitrogen (N_2) were studied via the CFD simulation through the MCM-41 nanoparticles - polysulfone (PSF) - MMMs. A three-dimensional MMM model with dimensions and parameters, as reported in Table 2, was constructed [12].

Th diffusivity and solubility parameters of CO_2, O_2, and N_2 in the PSF polymer matrix and the MCM-41 nanoparticles are given in Table 3 [12]. To create spheres as the filler particles with different diameters (d_f), an algorithm according to the Monte-Carlo method for the randomized positioning of each filler particle was employed [33]. Firstly, the number of randomly located filler particles was calculated. The employed program of MATLAB 2009 linked with COMSOL 5.2a resulted in the three dimensional randomly dispersed filler particles of 0.2, 4, and 8 μm in diameter in the cubic volume of 15 μm × 15 μm × 15 μm.

Table 2
Physical and geometrical parameters of the constructed MMM model [12].

Variable / Parameter	Unit	Size
Radius of MCM-41 nanoparticles	μm	0.1 - 4
Matrix height	μm	15
Matrix length	μm	15
Matrix width	μm	15
MCM-41 nnoparticles volume fraction	-	0 - 0.49

Table 3
Fickian diffusivity and solubility coefficients of penetrants in the PSF and MCM-41 particles at 308 K and 0.1 bar [12].

Penetrant	D (× 10^{-8}, cm^2/s)	S (× 10^{-2} cm^3(STP)/cm^3, cm Hg)	P = D × S (Barrer)	K = S_f / S_m	D_f / D_m
	MCM-41 nanoparticles				
CO_2	2040	2.50	5100	0.61	1854.0
O_2	125000	0.648	81000	2.20	37537.5
N_2	10.8	0.6	6.48	3.50	10.3
	PSF				
CO_2	1.1	4.09	4.499	-	-
O_2	3.33	0.294	0.97902	-	-
N_2	1.05	0.1714	0.17997	-	-

The constructed three-dimensional structure of the MMM was meshed by a tetrahedral mesh (Figure 1) and the Finite Element Method (FEM) was applied for solving the governing equations. The density resolution of the mesh was changed among the extremely fine, normal, and extremely coarse in COMSOL. The average mesh in 30 % loading of the filler particles was 134 $elements/\mu m^3$ for the filler phase and about 87 $elements/\mu m^3$ for the matrix. As shown in Table 4, the concentrations of CO_2, O_2, and N_2 at the MMM upper (feed) and lower (permeate) sides were considered to be 1 and 0 mol/m^3 respectively. Other boundary conditions are also given in Table 4.

a)

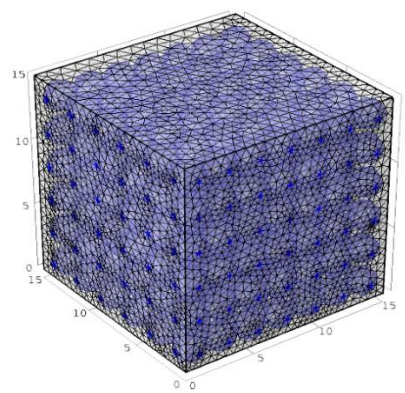

b)

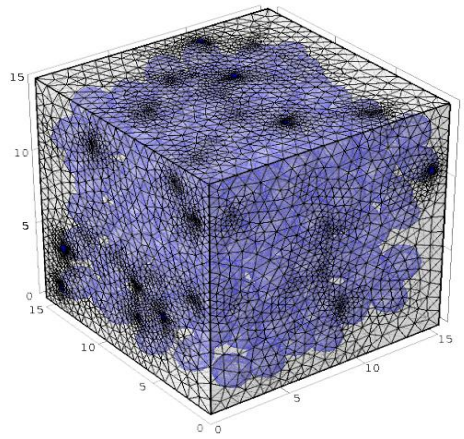

Figure 1. Constructed three-dimensional structure of the MMM by the Matlab program linked with COMSOL and meshed by tetrahedral meshes used in the simulation of randomly dispersed filler particles.

Table 4
Boundary conditions of the constructed of three-dimensional structural model for MMMs.

Boundary	Value	Boundary	Value
x = 0	$C_i = 1$	y, z = 0	No flux
x = l	$C_i = 0$	y, z = 1	No flux
Interface	$C_{i-m} = K * C_{i-f}$		

2.2. Computational methods

In the developed model, it was assumed that the transport of the penetrants occurred only by the diffusion mechanism in the steady state mode. All the species pass through the MMM due to the chemical potential differences across the membrane. As a result, only the Fick's first law Equation (1) describes the mass transport through the MMM. In other words, the membrane structure was considered as the ideal one, i.e., no structural defects [30]:

$$J_i = D_i \nabla C_i \tag{1}$$

where J_i, D_i, and ∇C_i are the molar flux, diffusivity coefficient, and concentration gradient of the ith penetrant. D can be the diffusion coefficient of the polymer (D_p), or of the filler particles (D_f), or that of effective for MMM (D_m). The mass conservation Equation inside the MMM in three dimensions can be written as [30]:

$$D_{i-membrane}\left[\frac{\partial^2 C_{i-membrane}}{\partial^2 x} + \frac{\partial^2 C_{i-membrane}}{\partial^2 y} + \frac{\partial^2 C_{i-membrane}}{\partial^2 z}\right] = 0 \tag{2}$$

After determining the penetrants' concentration profiles inside the MMMs using FEM, the effective diffusivity (D_{eff}) of the ith penetrant can be calculated using the following equation [29]:

$$D_{eff} = \frac{J_x . L}{C_{feed} - C_{permeate}} \tag{3}$$

where J_x is the mean surface molar flux in the x-direction from the feed side to the permeate side of the MMM, L is the thickness of the MMM in the mass transfer direction, and C_{feed} and $C_{permeate}$ are the concentrations of the ith penetrants at the feed and the permeate sides respectively [29]. The effective permeability of specie i through the MMM can be written as the following equation [31]:

$$P_{eff} = \frac{L[-D_{eff}(x)dC_{CO_2}/dx]}{RT(C_{feed}-C_{permeate})} = \frac{J_x L}{RT(-\Delta C_{CO_2})} \quad (4)$$

A two-dimensional schematic of one filler particle is incorporated in the MMM, penetrants permeate only in the x-direction while there is no permeation in the y- and z-directions, i.e., insulated boundaries (Figure 2). Meanwhile, the constructed structure was three-dimensional, and one-dimensional mass transfer was considered in the x-direction.

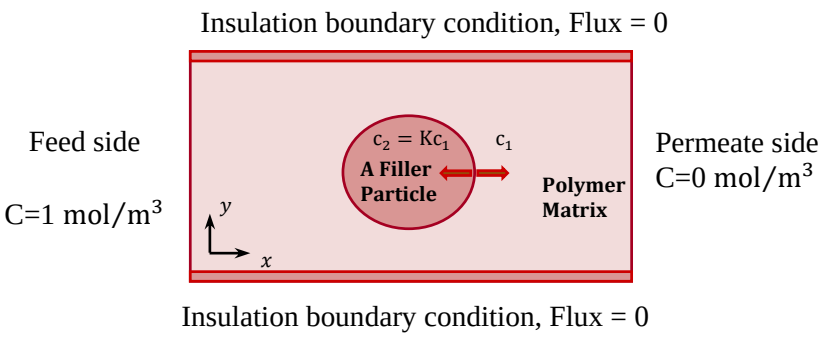

Figure 2. Two-dimensional schematic presentation of an MMM and its boundary conditions.

3. Results and discussion

The mesh number was changed regularly for the CFD simulation of the penetrants' permeation through the MMM. The mesh number and configuration should be selected in a manner to provide the simulation result(s) with an adequate level of precision and at the same time acceptable computation hardware and time requirements. Before performing all the tasks for the simulation, the independence of the simulated result in term of the ratio of D_{eff}/D_m was studied vs mesh No. as presented in Figure 3. All other simulation studies were carried out with mesh No. of 12456.

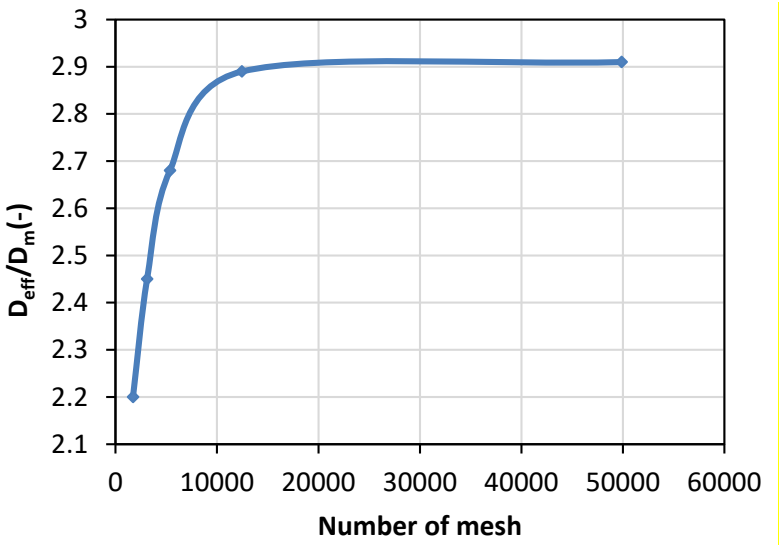

Figure 3. Effective MMM diffusion coefficient ratio (D_{eff}/D_m) vs. the structural mesh No.

The effective ratio of the diffusion coefficient of the MMM to that of the matrix (D_{eff}/D_m) vs. the filler volume fraction is plotted for the D_f/D_m = 100 using different permeability prediction models for MMMs, as shown in Figure 4. As it can be observed, the

current CFD simulation results show better fitness with the Maxwell and the Lewis-Nielsen models. The last one needs to be solved by the trial and error procedure for predicting the effective permeability [34].

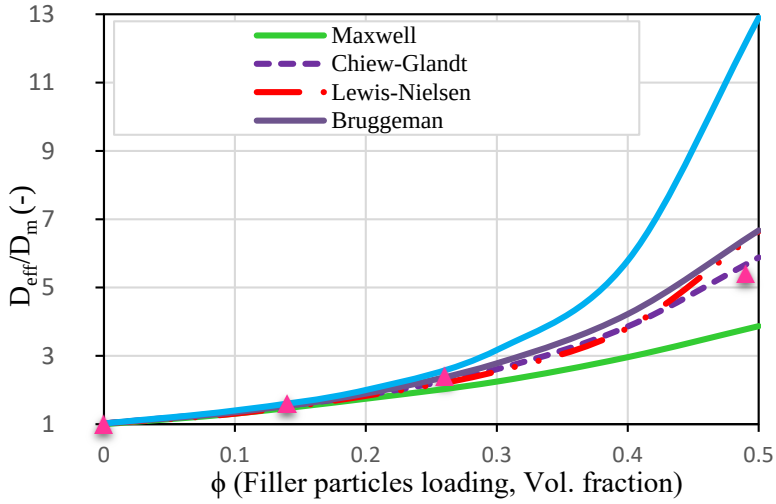

Figure 4. Prediction of the dimensionless effective diffusion coefficient of MMMs using famous predictive models and the current CFD simulation.

3.1. Comparison of the results of simulations with those of experiments

In this simulation, the intrinsic diffusivity and solubility ratios of the filler particles and the polymer matrix phases for three examined penetrants were used [12], and then the results were compared with the experimental data [12, 26]. The values of variables/parameters of the three examined penetrants are given in Table 3 and their comparisons are revealed in Figure 5, Figure 6, and Figure 7 respectively.

Figure 5 shows the simulation results and experimental data for CO_2, which are in an acceptable agreement in the low loadings of filler particles, i.e., AARE of 31.0 %. Also, Figure 6 and Figure 7 show the simulation results and experimental data for O_2 and N_2 respectively. As it can be observed, simulation results are properly fitted in the low loading of the filler particles, i.e., AARE of 42.7 % for O_2 and 41.0 % for N_2.

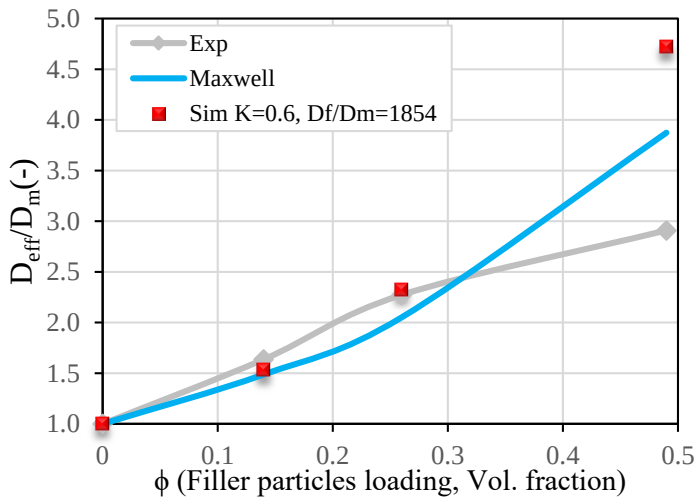

Figure 5. Comparison of the D_{eff}/D_m raio of the simulated CFD, the predicted Maxwell model, and the experimentally measured permeability of CO_2. Experimental data were gathered from Kim et al. [12].

However, there are some deviations between the estimated and experimental data of the ratio of D_{eff}/D_m versus the loading of filler particles which can be divided into two regions. Trends associated with the ratio of D_{eff}/D_m observed in the experiments by increasing the loading of filler particles can be attributed to the characteristics of the locally rigidified polymer chains' matrix of MMMs due to the incorporated filler particles. This fact that the rigidified regions of the polymer chains have not been considered in the current model, results in a relatively large deviation of the simulated data from that of the experimentally measured. Figure 6 and Figure 7 summarize O_2 and N_2 penetrant data [12, 26] which show a similar trend where the results of the CFD simulation agreed with those of experimental data, especially at the low loadings of filler particles.

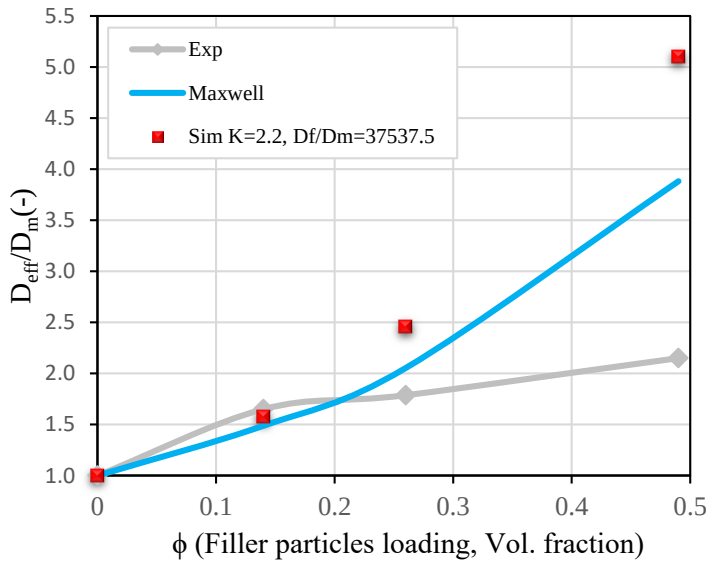

Figure 6. Comparison of the D_{eff}/D_m ratio of the simulated CFD, the predicted Maxwell model, and the experimentally measured permeability of O_2. Experimental data were gathered from Kim et al. [12].

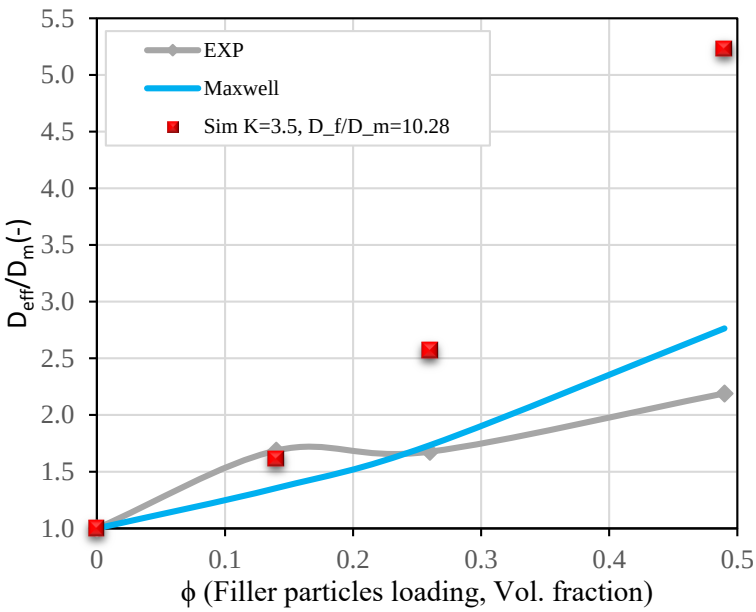

Figure 7. Comparison of the D_{eff}/D_m ratio of the simulated CFD, the predicted Maxwell model, and the experimentally measured permeability of N_2. Experimental data were gathered from Kim et al. [12].

Locally rigidifying polymer matrix chains may result in the reduction of the ratio of D_{eff}/D_m at the higher loading of filler particles. The rigidification of the polymeric matrix chain seems to be a common phenomenon that occurs in the preparation of MMMs; therefore, it is better to consider it via modeling with physically meaningful parameters that is being studied

Applying the reported boundary conditions and using proper mesh sizes, the concentration profiles of MMM inside the constructed structure were determined and are shown in Figure 8. The two-dimensional concentration profile in the x-y plane cut at z = 7 μm, as shown in Figure 9, is the characteristic of the grainy texture of the MMMs which is caused by the layering of the filler particles arrangement.

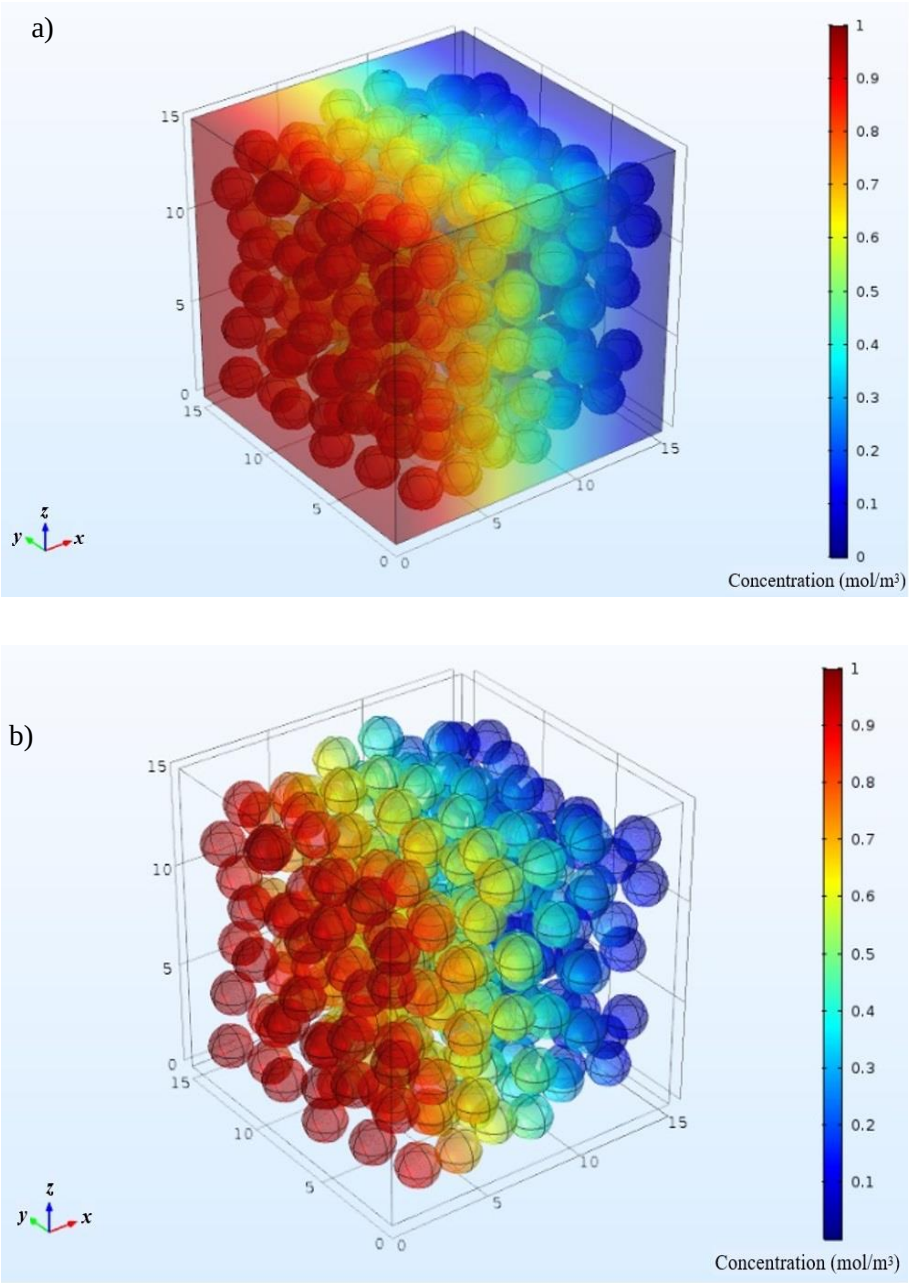

Figure 8. Determined concentration profiles of (a) the polymer matrix and (b) the filler particles of MMMs at a partition coefficient of K = 1.

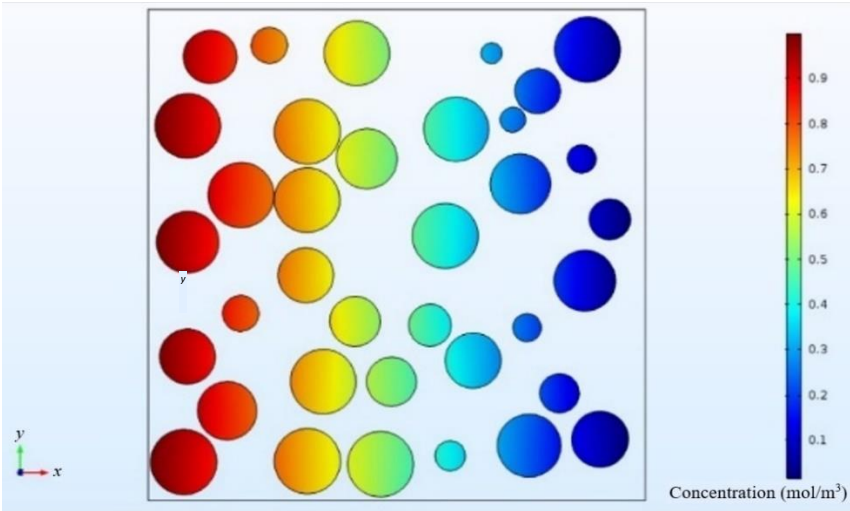

Figure 9. Two-dimensional concentration profiles in the x-direction of the mass transport across the MMM for K = 1.

3.2. Effect of the diffusivity ratio to the effective diffusivity ratio

The ratio of diffusivities of the filler particles to the polymer matrix is an important parameter that plays a role in the enhancement of the effectiveness the resultant MMM' diffusivity. To investigate the effect of this parameter, the constructed structure of the MMM was simulated by the K = 1 and different values of the D_f/D_m ratio. The D_{eff}/D_m values shown in Figure 10 include the minimum and maximum deviations in the three experimental data associated with different loadings of filler particles. As it is observed in Figure 10, at the low loadings of filler particles, the simulation results are in good agreement with those of the Maxwell model (AARE of about 31 %), however, as the loadings of filler particles are increased, the simulated CFD and other predictive models deviate significantly from the predictions by the Maxwell model. This deviation may be ascribed to the non-idealities, such as the rigidification of the polymer chain or void formation around the incorporated filler particles, that occurred in the MMM's structure [14].

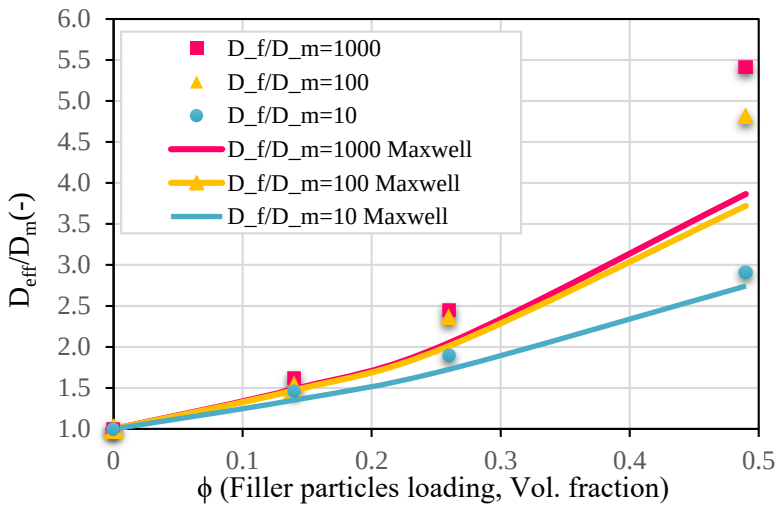

Figure 10. Effective ratio of the MMM diffusivity vs. the loading of filler particles for the simulated CFD results and the Maxwell model.

3.3. Effect of the solubility ratio

Similarly to the diffusivity parameter, solubility is also effective in the mass transfer through the membrane. To evaluate the effect of the solubility of the penetrant species in the polymer matrix and the filler particles phase, the solubility partition coefficient (K) between the polymer matrix and the filler particles is defined as follows:

$$C_f = KC_m \tag{5}$$

where C_f is the molar concentration of the filler particles and C_m is the molar concentration of the polymer matrix.

The effect of the solubility ratio on the D_{eff}/D_m ratio is shown in Figure 11. As it is observed, an increase in the K values has a larger impact on the enhancement of the D_{eff}/D_m ratio compared with that of the D_f/D_m ratio, which is quite consistent with the previously published results [27, 30, 31]. The effect of K values (K≠1) on the D_{eff}/D_m ratio was also investigated. The simulation for different combinations of the K values and D_f/D_m ratios, where the parameter K was constant and equal to 100, was performed. As Figure 11 shows, the lowest value of the D_{eff}/D_m ratio is obtained for K = 1.

Figure 11 compares the Maxwell results with the simulation results for different interface equilibrium constants. The above observation confirms that this behavior of the MMMs is different from that of MMMs estimated by EMT models for K ≠ 1. The deviation of the EMT results from the experimentally observed data may be because the EMT models consider the filler phase as the continuous phase.

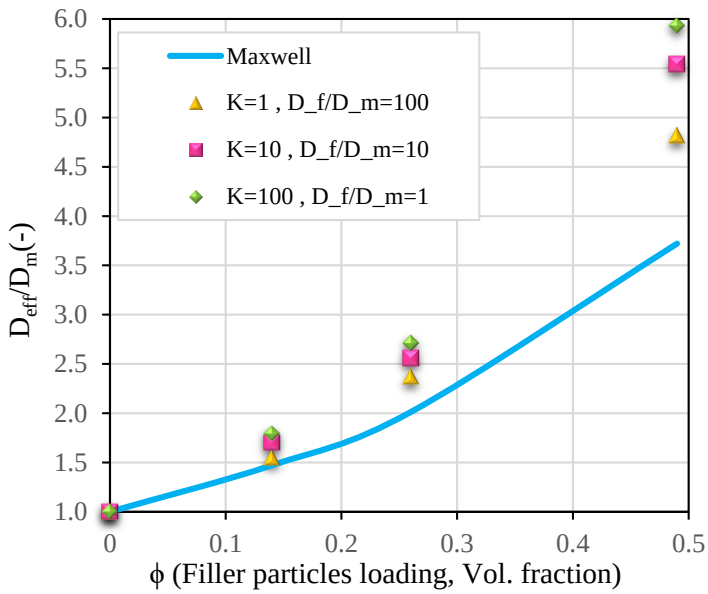

Figure 11. Comparison of the current simulation results and those of the Maxwell model for different K-values.

3.4. Effect of the particle size of fillers on the effective diffusivity of the MMM

Simulations and theories showed that increasing the particles size of the filler decreases the effective diffusivity ratio of MMMs [30, 31]. This effect may be attributed to a decrease in the interfacial contact on the surface area between the polymer matrix and the filler particles phases. In addition, the number of filler particles per unit volume decreases as their size increases at the constant volume fractions of the fillers. Furthermore,

the smaller particles size of the filler, will make the membrane thinner resulting in an increment in the of effective permeability of MMMs since the molar flux has an inverse relationship with the thickness of the membrane [31].

In the current study, the effective diffusivity ratios of MMMs were investigated for three different sizes (Table 2) of the filler particles and K = 1 as shown in Figure 12. As it is observed, a reduction in the particles size of the filler results in an increase in the D_{eff}/D_m ratio, which is consistent with the experimentally measured results [12].

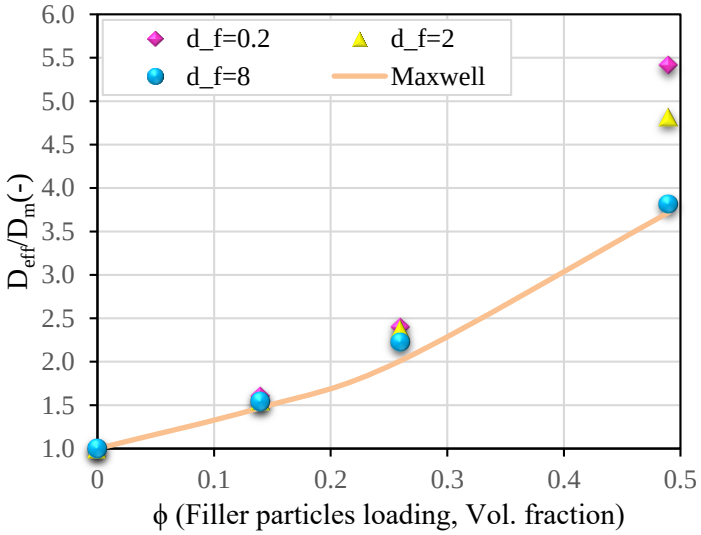

Figure 12. Impact of the particle size of the filler on the effective diffusivity (D_{eff}/D_m) of the MMM.

3.5. Effect of the packing structure of MMMs

Another parameter that can change the effective diffusivity of MMMs is the packing regularity or randomness of the incorporated filler particles. As it is revealed in Figure 13, MMMs with the filler particles randomly incorporated into the polymer matrix, at the same effective diffusivity, show higher permeability, which can be attributed to the longer diffusion path of the penetrants through the MMM. In other words, as the penetration tortuosity (τ) increases, it makes the membrane's performance better.

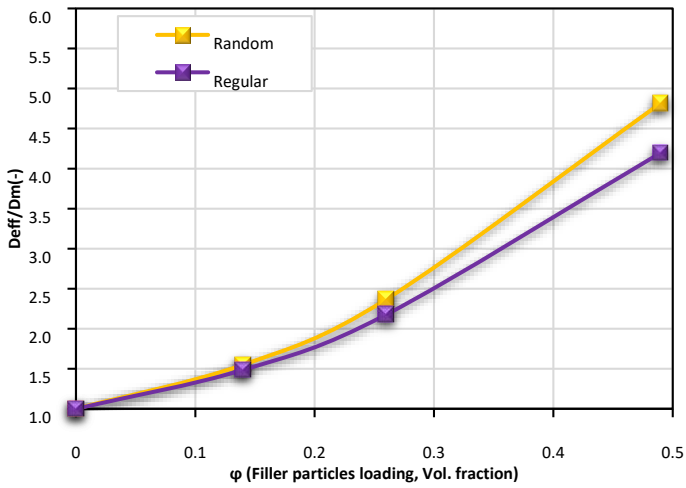

Figure 13. Effect of the packing regularity or randomness of the filler particles in the MMM structure on its D_{eff}/D_m ratio.

4. Conclusions

In the current study, a numerical method was developed, based on the steady state mass transfer in three-dimensional structure, and used for the CFD simulation of the effective diffusivity of MMMs. The effect of the parameters, such as the particle size of the filler, diffusivity, and solubility ratios of the polymer matrix and the particle phases of the filler were investigated. The results of the simulation showed that by increasing the solubility and diffusivity ratios, the effective diffusivity of the MMM increased for the ideal assumed structure of MMMs. According to the results, increasing the particle size of the filler decreases the effective diffusivity of the MMM due to the decline of the overall interfacial surface of the contact area. In addition, the results show that the effect of the parameter K is greater than that of the D_f/D_m ratio.

The CFD simulation results are in good agreement with the experimentally measured data, especially at the lower loadings of filler particles. The incompatibilities observed at the higher loadings of filler particles are probably due to the presence of non-idealities, such as the rigidification of the polymer chains or void formation around the incorporated filler particles, that may occur in the structure of MMMs which are not usually considered in the traditional predictive models such as Maxwell. So, the AARE of the CFD simulation of the gaseous effective diffusivity of CO_2 and the experimental ones measured by the Maxwell method were calculated as 31 and 19.5 % respectively. Those of O_2 were found as 42.7 and 33 % and for N_2 as 41 and 26 % respectively. the AAREs of the results of the current study are lower than almost all above cited researches indicting the ability of the correctly employed CFD tools to provide a better understanding of the realities of the actual MMMs' structure. Results show that the accurate prediction of the separation performance of MMMs requires more realistic access to the inherent role of absorption, penetration, and morphological properties of the MMMs in the evalaution of observed behaviors.

Nomenclature

P_c	continuous phase permeability [Barrer].
D	diffusion coefficient [$cm^2.s^{-1}$].
P_d	dispersed phase permeability [Barrer].
D_f/D_m	diffusivity ratio of filler particle to the matrix.
d_f	filler particles diameter [μm].
C	gas concentration [$mol.lit^{-1}$].
L	membrane thickness [μm].
J	molar fux [$mol.m^{-2}.s^{-1}$].
P_M	MMMs permeability [Barrer].
D_{eff}/D_m	MMMs effective diffusivity ratio to the matrix.
x y z	orientation directions [μm].
O	error order of magnitude.
K	partitioning coefficient.
p	pressure [kPa].
S	penetrant's solubility in the membrane [$cm^3(STP)/cm^3.cm\ Hg$].
S_f/S_m	solubility ratio of filler particle to the matrix.
T	temperature [K].
R	universal gas constant [$kJ/kmol.K$].
Greek letters	
ϕ_d	filler particles volume fraction.
θ	filler particles orientation angle [°].
ϕ_m	maximum filler particles volume fraction.
β	the Chiew - Glandt model parameter.
ψ	the Lewis - Nielsen model parameter.
ϕ	volume fraction of the dispersed phase.

References

[1] Baker, R. W., Membrane technology and applications, 2nd ed., John Wiley & Sons, New York, USA, p. 96 (2004).

[2] Banhegyi, G., "Comparison of electrical mixture rules for composites", *Colloid and Polymer Science*, **264** (12), 1030 (1986).

[3] Brunetti, A., Scura, F., Barbieri, G. and Drioli, E., "Membrane technologies for CO_2 separation", *Journal of Membrane Science*, **359** (1-2), 115 (2010).

[4] Freeman, B. and Yampolskii, Y., Membrane gas separation, John Wiley & Sons, USA, (2011).

[5] Robeson, L. M., "The upper bound revisited", *Journal of Membrane Science*, **320** (1-2), 390 (2008).

[6] Lin, H., van Wagner, E., Raharjo, R. and Freeman, B. D., "High-performance polymer membranes for natural-gas sweetening", *Advanced Materials*, **18** (1), 39 (2006).

[7] Sen, S. K., Dasgupta, B. and Banerjee, S., "Effect of introduction of heterocyclic moieties into polymer backbone on gas transport properties of fluorinated poly (ether imide) membranes", *Journal of Membrane Science*, **343** (1-2), 97 (2009).

[8] Ahn, J., Chung, W. -J., Pinnau, I. and Guiver, M. D., "Polysulfone/silica nanoparticle mixed-matrix membranes for gas separation", *Journal of Membrane Science*, **314** (1), 123 (2008).

[9] Kim, S., Pechar, T. W. and Marand, E., "Poly (imide siloxane) and carbon nanotube mixed matrix membranes for gas separation", *Desalination*, **192** (1-3), 330 (2006).

[10] Zhang, Y., Balkus Jr., K. J., Musselman, I. H. and Ferraris, J. P., "Mixed-matrix membranes composed of Matrimid® and mesoporous ZSM-5 nanoparticles", *Journal of Membrane Science*, **325** (1), 28 (2008).

[11] Hosseini, S. F., "Enhanced gas separation performance of nanocomposite membranes using MgO nanoparticles", *Journal of Membrane Science*, **302** (1-2), 207 (2007).

[12] Kim, S. and Marand, E., "High permeability nano-composite membranes based on mesoporous MCM-41 nanoparticles in a polysulfone matrix", *Microporous and Mesoporous Materials*, **114** (1), 129 (2008).

[13] Nik, O. G., Chen, X. Y. and Kaliaguine, S., "Amine-functionalized zeolite FAU/EMT-polyimide mixed matrix membranes for CO_2/CH_4 separation", *Journal of Membrane Science*, **379** (1), 468 (2011).

[14] Aroon, M. A., Ismail, A. F., Matsuura, T. and Montazer-Rahmati, M. M., "Performance studies of mixed matrix membranes for gas separation: A review", *Separation and Purification Technology*, **75** (3), 229 (2010).

[15] Chung, T. -S., Jiang, L. Y., Li, Y. and Kulprathipanja, S., "Mixed matrix membranes (MMMs) comprising organic polymers with dispersed inorganic fillers for gas separation", *Progress in Polymer Science*, **32** (4), 48 (2007).

[16] Bastani, D., Esmaeili, N. and Asadollahi, M., "Polymeric mixed matrix membranes containing zeolites as a filler for gas separation applications: A review", *Journal of Industrial and Engineering Chemistry*, **19** (2), 375 (2013).

[17] Mahajan, R., "Formation, characterization and modeling of mixed matrix membrane materials", University of Texas at Austin, (2000).

[18] Maxwell, J., Electricity and magnetism, Clarendon Press, Oxford, UK, (1873).

[19] Bruggeman, D. A. G., "Berechnung verschiedener physikalischer Konstanten von heterogenen Substanzen. III. Die elastischen Konstanten der quasiisotropen Mischkörper aus isotropen Substanzen", *Annalen der Physik*, **421** (2), 160 (1937).

[20] Lewis, T. B. and Nielsen, L. E., "Dynamic mechanical properties of particulate-filled composites", *Journal of Applied Polymer Science*, **14** (6), 1449 (1970).

[21] Pal, R., "New models for thermal conductivity of particulate composites", *Journal of Reinforced Plastics and Composites*, **26** (7), 643 (2007).

[22] Chiew, Y. and Glandt, E., "The effect of structure on the conductivity of a dispersion", *Journal of Colloid and Interface Science*, **94** (1), 90 (1983).

[23] Davis, H., Valencourt, L. and Johnson, C., "Transport processes in composite media", *Journal of the American Ceramic Society*, **58** (9-10), 446 (1975).

[24] Davis, H. T., "The effective medium theory of diffusion in composite media", *Journal of the American Ceramic Society*, **60** (11-12), 499 (1977).

[25] Landauer, R., "The electrical resistance of binary metallic mixtures", *Journal of Applied Physics*, **23** (7), 779 (1952).

[26] Marand, E. and Surapathi, A., "The role of solubility partition coefficient at the mixed matrix interface in the performance of mixed matrix membranes", *Journal of Membrane Science*, **415** (Supplement C), 871 (2012).

[27] Singh, T., Kang, D. -Y. and Nair, S., "Rigorous calculations of permeation in mixed-matrix membranes: Evaluation of interfacial equilibrium effects and permeability-based models", *Journal of Membrane Science*, **448** (Supplement C), 160 (2013).

[28] Gheimasi, K. M., Mohammadi, T. and Bakhtiari, O., "Using a new model for prediction of gas permeability through MMMs: Considering effects of particles shape, polymer chain rigidification, partial pore blockage, and void formation", *Separation Science and Technology*, **50** (15), 2384 (2015).

[29] Wang, T. -P. and Kang, D. -Y., "Predictions of effective diffusivity of mixed matrix membranes with tubular fillers", *Journal of Membrane Science*, **485**, 123 (2015).

[30] Yang, A. -C., Liu, C. -H. and Kang, D. -Y., "Estimations of effective diffusivity of hollow fiber mixed matrix membranes", *Journal of Membrane Science*, **495** (Supplement C), 269 (2015).

[31] Monsalve-Bravo, G. M. and Bhatia, S. K., "Extending effective medium theory to finite size systems: Theory and simulation for permeation in mixed-matrix membranes", *Journal of Membrane Science*, **531** (Supplement C), 148 (2017).

[32] Rajati, H., Bakhtiari, O. and Mohammadi, T., "Molecular modeling of the gaseous penetrants permeabilities through 4A, DDR and silicalite-1 zeolites incorporated in mixed matrix membranes", *Separation Science and Technology*, **53** (6), 910 (2018).

[33] Tilton, G. J., "Finite element modeling of thermal expansion in polymer/ZrW_2O_8 composites", University of Toledo, (2011)

[34] Pal, R., "Permeation models for mixed matrix membranes", *Journal of Colloid and Interface Science*, **317** (1), 191 (2008).